EMITTANCE AND PHASE SPACE EXCHANGE*

Dao Xiang† and Alex Chao, SLAC, Menlo Park, CA, 94025, USA

Abstract

Alternative chicane-type beam lines are proposed for exact emittance exchange between horizontal phase space (x, x') and longitudinal phase space (z, δ). Methods to achieve exact phase space exchanges, i.e. mapping x to z, x' to δ, z to x and δ to x' are suggested. Methods to mitigate the thick-lens effect of the transverse cavity on emittance exchange are discussed. Some applications of the phase space exchanger and the feasibility of an emittance exchange experiment with the proposed chicane-type beam line at SLAC are discussed.

EMITTANCE EXCHANGE

Consider a planar lattice that allows coupling between x- and z-motions. Let the coordinate vector be $(x, x', z, \delta)^T$. Consider a transport section whose transport matrix from entrance to exit is

$$\begin{bmatrix} A & B \\ C & D \end{bmatrix}, \tag{1}$$

where A, B, C and D are 2×2 matrices. Exact emittance exchange (EEX) is achieved when the elements in A and D are all zeros. This special transport section has the property that it cleanly exchanges the (x, x') and the (z, δ) degrees of freedom.

The first beam line [1] proposed for EEX is shown in Fig. 1. It consists of a simple 4-bend chicane and a transverse cavity.

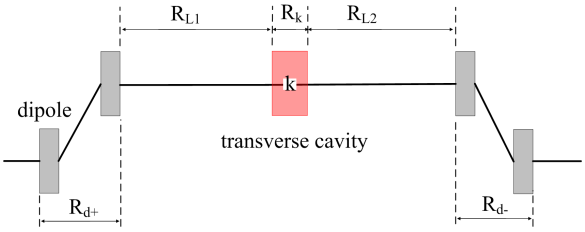

Figure 1: Cornacchia-Emma's EEX beam line.

The transfer matrix for the whole beam line is $R_1 = R_{d-}R_{L_2}R_kR_{L_1}R_{d+}$, where R_{d+} and R_{d-} are the transfer matrices for the first and second half of the chicane, R_{L_1} and R_{L_2} are the transfer matrices for the drifts before and after the transverse cavity, and R_k is the transverse cavity transfer matrix. Partial EEX is achieved when $\eta k = 1$, where η is the dispersion in the center of the chicane and $k = 2\pi eV/\lambda E$ is the dimensionless deflection strength of the transverse cavity, V is the deflection voltage, λ is the wavelength of the rf field and E is the electron energy. However, the EEX is not complete in this beam line because there are non-zero elements in A and D.

An exact exchange optics was later proposed by K.-J. Kim [2]. Instead of a chicane, the transverse cavity is put between two identical doglegs. The transfer matrix for this beam line is $R_2 = R_{d+}R_{L_2}R_kR_{L_1}R_{d+}$. Exact EEX is achieved when $\eta k = -1$. Based on this optics, experiments at FNAL [3] have been performed and others are being planned at ANL [4].

EEX WITH A CHICANE-TYPE BEAM LINE

From a practical point of view, EEX with a chicane may be more desirable because of its simplicity, wide availability and minimal perturbation to existing beam lines (e.g. it does not introduce offset in beam trajectory and turning off the transverse cavity allows dispersion to return to zero). But it has a lower performance compared to the two-dogleg scheme. Here we show that the chicane scheme can achive exact EEX as well by adding (at least two) quadrupoles. The scheme is shown in Fig. 2.

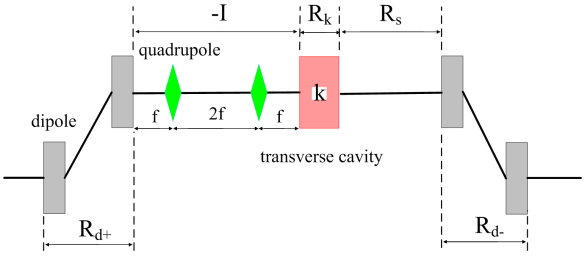

Figure 2: A chicane-type exact EEX beam line.

Two quadrupoles together with three drifts are used to form a negative unity transfer matrix for the transverse plane. The focal lengths of the two quadrupoles are both f. With the lengths of the drifts chosen as shown in Fig. 2, the transfer matrix for the $-I$ section is $R_{-I} = \begin{bmatrix} -I & 0 \\ 0 & I \end{bmatrix}$. The negative unity section reverses the dispersion of the first half of the chicane, which is optically equivalent to flipping the sign of a dogleg. The transfer matrix for the whole beam line ($R_c = R_{d-}R_SR_kR_{-I}R_{d+}$) when $\eta k = 1$ is,

$$R_c = \begin{bmatrix} 0 & 0 & k(L+S) & k\xi(L+S) - \eta \\ 0 & 0 & k & k\xi \\ -k\xi & \eta - kL\xi & 0 & 0 \\ -k & -kL & 0 & 0 \end{bmatrix}, \tag{2}$$

* Work supported by US DOE contracts DE-AC02-76SF00515.

† dxiang@slac.stanford.edu

where L, ξ and η are the length, the momentum compaction and dispersion of the first half of the chicane. Equation (2) implies that such a beamline also provides exact exchange for the transverse and longitudinal emittances. Further analysis shows that the angular to spatial element for the transfer matrix R_{-I} does not need to be zero for an exact exchange, which indicates that the distance between the negative unity matrix beam line and the deflecting cavity can be arbitrary. Also the R_{-I} section can be put downstream of the deflecting cavity, for which case exact EEX can be achieved with $\eta k = -1$.

PHASE SPACE EXCHANGE

It follows from Eq. (2) that $z_f = -k\xi x_i + (\eta - kL\xi)x_i'$ and $\delta_f = -kx_i - kLx_i'$. Therefore, by shaping the initial transverse phase space (x_i, x_i'), the final longitudinal phase space distribution (z_f, δ_f) can be tailored. Note it is easy to shape the x distribution using masks with various shapes, but shaping x' distribution can be technically challenging. In practice one can always make the final z_f and δ_f dominated by initial x_i other than x_i', so that shaping x distribution suffices. This is typically achieved by properly choosing the parameters for the EEX beam line and increasing the beam size at the entrance to the EEX beam line. Experiments at FNAL have demonstrated that one can generate sub-ps bunch train by modulating the initial transverse distribution with multi-slits [5]. However, the cross-term dependences of z_f and δ_f on x_i and x_i' may set a limit on how well the phase space can be tailored.

Here we show further that by adding more quadrupoles upstream and downstream of the beam line in Fig. 2, we can achieve exact phase space exchange (PSEX), i.e. mapping x to z, x' to δ, z to x, and δ to x'. This allows more advanced surgery for beam phase space manipulation.

For the system that provides exact EEX, its transfer matrix has the form $\begin{bmatrix} 0 & B \\ C & 0 \end{bmatrix}$. We now add a section consisting of drifts and quadrupoles in front, and another similar section after the exchanger beam line. Let these two sections' 4×4 transport matrices be $\begin{bmatrix} E & 0 \\ 0 & I \end{bmatrix}$ and $\begin{bmatrix} F & 0 \\ 0 & I \end{bmatrix}$ respectively, where I is a 2×2 unit matrix and E and F are some other general 2×2 matrices with unit determinants.

The total transport matrix is then

$$\begin{bmatrix} F & 0 \\ 0 & I \end{bmatrix} \begin{bmatrix} 0 & B \\ C & 0 \end{bmatrix} \begin{bmatrix} E & 0 \\ 0 & I \end{bmatrix} = \begin{bmatrix} 0 & FB \\ CE & 0 \end{bmatrix} \quad (3)$$

By lattice matching using the two drift-quadrupole sections, it is possible to create arbitrary results for FB and CE to meet the desired lattice properties. For example, if we design the two drift-quadrupole sections such that $F = B^{-1}$ and $E = C^{-1}$ then we would have a transport line that has a transport matrix $\begin{bmatrix} 0 & I \\ I & 0 \end{bmatrix}$, i.e. it will map x to z, x' to δ, z to x, and δ to x'. It is worth pointing out that mapping x to δ, x' to z, and/or z to x', and δ to x are all also possible, but they will have opposite sign, i.e. when x is mapped to δ, x' will be mapped to $-z$.

Exact phase space exchange may have wide applications. For instance, by mapping z exactly to x, the beam's temporal structures can be easily measured with a view screen. By mapping x exactly to z, to the first order, one may generate bunch trains with arbitrary spacing, which might be beneficial for future FELs [6].

THICK-LENS EFFECTS

The thick-lens transfer matrix of a deflecting cavity is

$$R_{k,thick} = \begin{bmatrix} 1 & L_c & kL_c/2 & 0 \\ 0 & 1 & k & 0 \\ 0 & 0 & 1 & 0 \\ k & kL_c/2 & k^2L_c/4 & 1 \end{bmatrix}, \quad (4)$$

where L_c is the length of the cavity. When the finite length of the deflecting cavity is taken into account, EEX as Fig. 2 based on thin-lens magnets is incomplete and the final projected emittances become

$$\epsilon_{x,z}^2 = \epsilon_{z0,x0}^2 + \frac{\epsilon_{x0}\epsilon_{z0}k^2L_c^2\gamma_{x0}}{16\beta_{z0}}[\xi^2 + (\beta_{z0} - \alpha_{z0}\xi)^2] \quad (5)$$

Since the second term in Eq. (5) scales as L_c^2, the simplest way to mitigate the thick-lens effect may be to reduce the cavity length. In the thin-lens approximation, the deflecting cavity only introduces $x' - z$ and $x - \delta$ correlation. But when the finite length is taken into account, it also introduces $x' - x$, $x' - \delta$, $z - z$ and $z - \delta$ correlations that lead to non-exact EEX. Intuitively, one can also reduce the values of x' and z at the cavity to mitigate the degradations from these additional correlations. For instance, by minimizing γ_{x0} and letting $\alpha_{z0} = \beta_{z0}/\xi$, the beam divergence and bunch length at the transverse cavity can be minimized, which also mimimizes the degradation from the finite length of the cavity. However, it should be pointed out that minimizing the bunch length at the cavity may cause serious CSR effect that can significantly degrade the EEX performance [2], especially when one tries to exchange the large transverse emittance with small longitudinal emittance.

While the thick-lens transfer matrix has non-zero R_{12}, R_{13}, R_{42} and R_{13} elements, analysis shows that the incomplete EEX is solely caused by the R_{43} term. Using a simple rf cavity in the fundamental mode to cancel the longitudinal acceleration in the transverse cavity may allow exact EEX when the finite length of the cavity is taken into account [7].

EEX WITH $|\eta K| \neq 1$

In all the beam lines discussed above, EEX requires $|\eta k| = 1$, where η is the dispersion of the dogleg. This condition makes EEX difficult to apply for high energy beams where either a huge dogleg with very large η or a long transverse cavity with very high voltage is needed to

satisfy the condition. Here we want to point out that the dispersion of the dogleg does not necessarily need to match the strength of the transverse cavity for EEX. We will show below that by adding telescope beam lines before and after the transverse cavity, the condition $|\eta k| = 1$ can be relaxed.

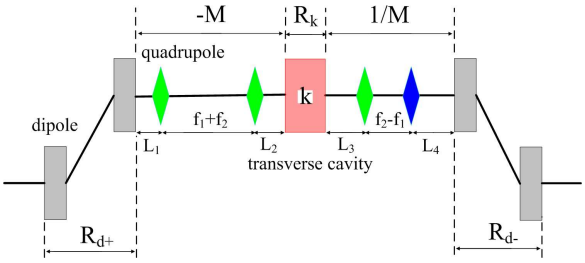

Figure 3: Exact EEX beam line with $|\eta k| < 1$.

As shown in Fig. 3, two focusing quadrupoles (green diamonds) are put upstream of the transverse cavity to form a telescope that magnifies the beam with a magnification ratio M, which also increases the local dispersion in the transverse cavity to $M\eta$. The transfer matrix is $\begin{bmatrix} R_{-M} & 0 \\ 0 & I \end{bmatrix}$, where $R_{-M} = \begin{bmatrix} -M & a \\ 0 & -1/M \end{bmatrix}$. After the transverse cavity, one focusing quadrupole and one defocusing quadrupole (blue diamond) are used to restore the beam to its initial size. The transfer matrix for this section is $\begin{bmatrix} R_{1/M} & 0 \\ 0 & I \end{bmatrix}$, where $R_{1/M} = \begin{bmatrix} 1/M & b \\ 0 & M \end{bmatrix}$. In R_{-M} and $R_{1/M}$, a and b depend on the drift lengths before and after the quadrupoles, but they do not affect the condition to achieve exact EEX. It is straightforward to prove that exact EEX for such a beam line is achieved when $\eta k = 1/M$. Note $M\eta$ is the local dispersion in the transverse cavity, so the the general requirement for EEX that the dispersion in the transverse cavity should equal to the inverse of the cavity strength still holds [8].

Note the second term in Eq. (5) scales as $k^2 L_c^2 \sim M^{-4}$, therefore by having $M > 1$, shorter transverse cavity with lower deflection voltage can be used in EEX which may greatly mitigate the thick-lens effects. On the other hand, for given deflection voltage and dispersion of the dogleg, EEX can be implemented at higher beam energy.

EEX AT NLCTA

A chicane integrated with 12 quadrupoles is available at the next linear collider test accelerator (NLCTA) at SLAC. An X-band deflecting cavity, originally installed for heating the beam slice energy spread to facilitate demonstration of the echo-enabled harmonic generation technique [9], is also available. Three of the quadrupoles between the second and third dipoles can be used to form the $-I$ section and an EEX experiment using the chicane-type exchange scheme is being planned at NLCTA.

Nearly complete EEX with the chicane-type exchanger beam line at NLCTA, has been simulated with ELEGANT [10] including the thick-lens effect ($L_c = 0.09$ m) and second order optics effects. The initial emittances are $\epsilon_{n,x0} = 3.00$ μm, $\epsilon_{n,z0} = 0.30$ μm and the final emittances after exchange is $\epsilon_{n,x1} = 0.32$ μm, $\epsilon_{n,z1} = 3.02$ μm. The growth in the final horizontal emittances is mainly from thick-lens effect and second order effects. CSR has not been included in this simulation.

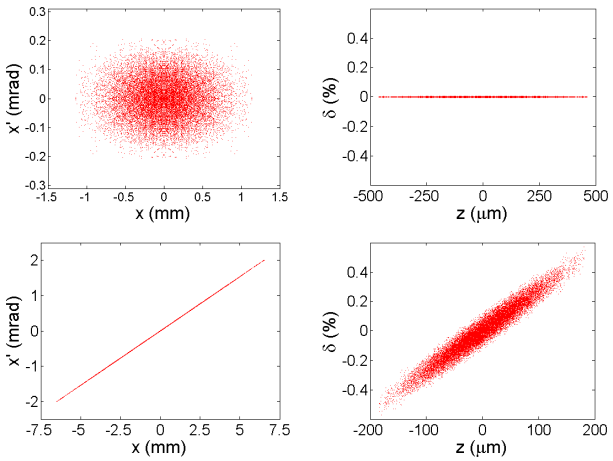

Figure 4: Transverse phase space distribution (left plots) and longitudinal phase space distribution (right plots) before (top row) and after (bottom row) EEX beam line.

When the telescope beam line is used with $M = 3$, the deflection voltage is reduced by a factor of 3, which results in a final horizontal emittance of $\epsilon_{n,x1} = 0.31$ μm. Now the emittance growth is mainly from the second order effects. We plan to test EEX with $|\eta k| \neq 1$ at NLCTA in the future.

REFERENCES

[1] M. Cornacchia and P. Emma, Phys. Rev. ST Accel. Beams, 5, 084001 (2002).

[2] P. Emma, Z. Huang, K.-J. Kim, and P. Piot, Phys. Rev. ST Accel. Beams, 9, 100702 (2006).

[3] J. Ruan *et al.*, *First observation of the exchange of transverse and longitudinal emittances*, http://arxiv.org/abs/1102.3155.

[4] Y.-E Sun *et al.*, Proceedings of PAC07, p.3441 (2007).

[5] Y.-E Sun *et al.*, Phys. Rev. Lett, 105, 234801 (2010).

[6] S.J. Russell *et al.*, Proceedings of PAC09, TH5PFP036, (2009).

[7] A. Zholents and M. Zolotorev, *New type of a bunch compressor and generation of a short wave length coherent radiation*, LBNL CBP Seminar, (2010).

[8] R. Fliller, Fermilab report BeamDocs 2271-v2, (2007).

[9] D. Xiang *et al.*, Phys. Rev. Lett, 105, 114801 (2010).

[10] M. Borland, "Elegant: A flexible SDDS-compliant code for accelerator simulation," Advanced Photon Source LS-287, September, (2000).